


Towards patterned bioelectronics: facilitated immobilization of exoelectrogenic *Escherichia coli* with heterologous pili

Michael Lienemann,^{1,*}  Michaela A. TerAvest,^{2,3}
Juha-Pekka Pitkänen,^{1,4} Ingmar Stuns,¹
Merja Penttilä,¹ Caroline M. Ajo-Franklin^{3,†} and
Jussi Jäntti^{1,†}

¹VTT Technical Research Centre of Finland Ltd, Espoo, Finland.

²Department of Biochemistry and Molecular Biology, Michigan State University, East Lansing, MI, USA.

³The Molecular Foundry, Lawrence Berkeley National Laboratory, Molecular Biophysics and Integrated Bioimaging Division, Synthetic Biology Institute, Berkeley, CA, USA.

⁴Current affiliation: Solar Foods Ltd, Helsinki, Finland.

Summary

Biosensors detect signals using biological sensing components such as redox enzymes and biological cells. Although cellular versatility can be beneficial for different applications, limited stability and efficiency in signal transduction at electrode surfaces represent a challenge. Recent studies have shown that the Mtr electron conduit from *Shewanella oneidensis* MR-1 can be produced in *Escherichia coli* to generate an exoelectrogenic model system with well-characterized genetic tools. However, means to specifically immobilize this organism at solid substrates as electroactive biofilms have not been

tested previously. Here, we show that mannose-binding Fim pili can be produced in exoelectrogenic *E. coli* and can be used to selectively attach cells to a mannose-coated material. Importantly, cells expressing *fim* genes retained current production by the heterologous Mtr electron conduit. Our results demonstrate the versatility of the exoelectrogenic *E. coli* system and motivate future work that aims to produce patterned biofilms for bioelectronic devices that can respond to various biochemical signals.

Introduction

Extracellular electron transfer (EET) is a biochemical process during which electrons are transferred across the bacterial cell envelope (White *et al.*, 2016). EET holds great potential for application in biosensing applications (PrévotEAU and Rabaey, 2017) where EET-performing cells represent an attractive alternative to less stable enzymes as sensing elements. Such biosensors contain the biological sensing element immobilized on a conductive surface where it performs the transduction of a specific chemical signal into an electric output. The capability of certain microbial species to reduce solid minerals at their surface allows their cultivation at the anode of a bioelectrochemical system (BES) and their genetic modification paved the way for their application in bioprocess and environmental monitoring (Webster *et al.*, 2014; PrévotEAU and Rabaey, 2017). In sensing applications, EET is utilized as a signal transducing process that, although slower than enzyme catalysts, is attractive when longevity, production costs, electric connection of the biological component, sensitivity and simultaneous processing of several signals are important.

Three decades ago, EET was discovered as manganese and iron respiration in species of *Geobacter* and *Shewanella* (Lovley and Phillips, 1988; Lovley, 1991; Marsili *et al.*, 2008a). More than 90 species have been reported to perform EET (Koch and Harnisch, 2017) including the EET model organisms *Geobacter sulfurreducens* and *Shewanella oneidensis*. Both species gain chemical energy in the form of ATP by coupling carbon oxidation to anaerobic reduction of metal oxide minerals such as Mn(III), Mn(IV), Fe(III), Cr(VI) and U(IV) in the

Received 20 March, 2018; revised 2 July, 2018; accepted 7 August, 2018.

*For correspondence. E-mail michael.lienemann@vtt.fi; Tel. +358 20 722 7153; Fax +358 20 722 7001.

†Denotes equal contribution.

Microbial Biotechnology (2018) 11(6), 1184–1194
doi:10.1111/1751-7915.13309

Funding Information

This research has been financially supported through the VTT Frontier Programme, the Biosolar programme granted by Tekes – the Finnish Funding Agency for Innovation (Diary No. 2299/31/2012; Decision No. 40044/13) and the Academy of Finland through a postdoctoral research grant (Decision No. 277121 to ML) and research grants SYNECO2 (Decision No. 272569 to JJ) and OPTOBIO (Decision No. 287011 to MP). Work at the Molecular Foundry was supported by the Office of Science, Basic Energy Sciences programme of the U.S. Department of Energy (Contract No. DE-AC02-05CH11231). CMAF and MAT acknowledge support from Office of Naval Research (Award number N000141310551).

extracellular space (Richter *et al.*, 2012). Despite the considerable number of reported electroactive microbes, the composition of their extracellular electron transfer pathway has remained largely unknown and is still limited to a small number of anode-respiring bacteria (Kracke *et al.*, 2015). In *S. oneidensis*, EET is initiated at the inner cell membrane where electrons, originating from the oxidation of primary fermentation products (e.g. lactate, pyruvate, formate and hydrogen), are transferred to membrane-embedded menaquinols by formate and NADH dehydrogenases (Meshulam-Simon *et al.*, 2007; Pinchuk *et al.*, 2009; Cordova *et al.*, 2011; Brutinel and Gralnick, 2012a; Kane *et al.*, 2016). Menaquinol is in turn oxidized by the inner membrane-bound quinol dehydrogenase CymA (Marriott *et al.*, 2012), or in its absence, the enzyme complex SirCD (Cordova *et al.*, 2011). Next, electrons are transferred across the periplasmic space by diffusible *c*-cytochromes STC and FccA (Schuetz *et al.*, 2009; Fonseca *et al.*, 2013) and transferred to terminal reductases at the outer membrane such as MtrA and MtrC which are associated with the MtrCAB complex (Fig. 1) (Coursolle and Gralnick, 2010; Breuer *et al.*, 2015). On the extracellular face of the outer membrane, MtrC accepts electrons from MtrA and transfers these charges either directly onto an insoluble electron acceptor or onto secreted flavin molecules (Brutinel and Gralnick, 2012b; Xu *et al.*, 2016).

Several research groups have used current knowledge on extracellular respiration to engineer non-natural

exoelectrogens by synthetic biology methods (TerAvest and Ajo-Franklin, 2016). Among these, the transfer of the EET capacity of *S. oneidensis* into the well-studied gene expression host *E. coli* has been explored in several studies (Pitts *et al.*, 2003; Gescher *et al.*, 2008; Jensen *et al.*, 2010; Goldbeck *et al.*, 2013; TerAvest *et al.*, 2014; Sturm-Richter *et al.*, 2015; Förster *et al.*, 2017). One such EET system was developed recently by Jensen *et al.*, who have incorporated the *S. oneidensis* inner membrane *c*-cytochrome CymA and the outer membrane complex MtrCAB into *E. coli* yielding the strain *cymAmtrCAB* (Jensen *et al.*, 2016). Remarkably, this strain was able to transfer electrons across the cell envelope in the absence of the periplasmic *S. oneidensis* cytochromes STC and FccA. Since CymA can reduce MtrA *in vitro* (Firer-Sherwood *et al.*, 2011), Jensen *et al.* proposed that the electrons transit the ~15 nm wide *E. coli* periplasm (Matias *et al.*, 2003) by diffusion of periplasmic MtrA. Hence, the four *S. oneidensis* MR-1 proteins CymA and MtrCAB form a functional Mtr electron transfer pathway (METP) in *E. coli* and were employed in the present study as a membrane-bound electron conduit. Electroactive *E. coli* strains such as *cymA-mtrCAB* differ from naturally occurring electroactive species in that the currently available exoelectrogenic *E. coli* strains neither form cohesive biofilms on electrodes nor utilize efficient extracellular electron transport mediators such as conductive pili or flavins. When considering strict anaerobic exoelectrogenic species such as *G. sulfurreducens*, the oxygen tolerance of *E. coli* can be regarded as a desirable feature as it may facilitate its incorporation in novel type of bioelectronics that are usually handled under ambient conditions. In addition, the use of non-biofilm-forming cells in electrochemical biosensors is complicated by complex chemical or physical immobilization and, in the case of biofilm-forming species, low reproducibility, required initial growth time and limited strain availability have to be considered during sensor design (PrévotEAU and Rabaey, 2017).

In order to further increase the relevance of the electroactive biological cell to bioelectronic applications, it is necessary to develop strains that can be stably and selectively immobilized at conductive substrates *in situ*. This may be done by, for instance, patterning of a biosensor surface with a synthetic biofilm consortium that can detect and process multiple signals in parallel. The attachment of current-producing bacteria on conductive surfaces was attempted previously using gold-binding peptides that were integrated with an *E. coli* outer membrane protein and displayed on the outer surface of *S. oneidensis* (Kane *et al.*, 2013). This system failed to maintain current production while introducing binding and, thereby, no strategy is currently available for

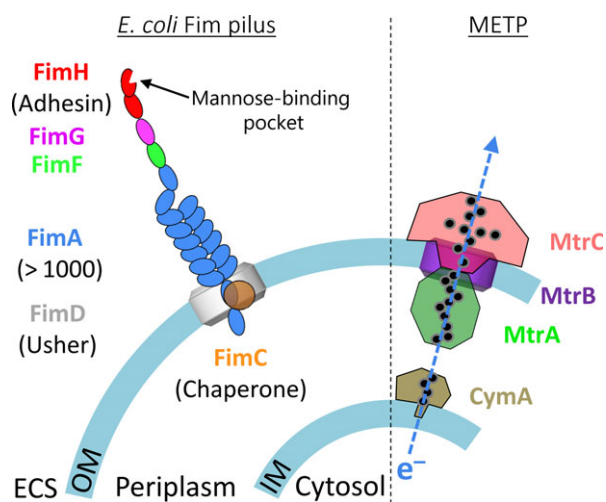


Fig. 1. Schematic of cell envelope of the constructed *E. coli* system. Fim pili are attached to the outer membrane (OM) and *S. oneidensis* MR-1 Mtr electron transfer pathway (METP) components are associated with outer and inner membrane (IM). Electron-conducting haem cofactors are displayed as filled black circles. The mechanism through which electrons are exchanged between IM-bound CymA and OM-bound MtrA is currently not known, but it is speculated that MtrA may participate in periplasmic electron transfer based on the observation of MtrA in the periplasmic compartment (Jensen *et al.*, 2016).

achieving patterning with exoelectrogenic bacteria. The specific and strong attractive interactions that are required for such an attachment are naturally provided by rod-like carbohydrate-binding cell appendages called pili (Fig. 1). These protein structures are naturally produced by, for example, uropathogenic *E. coli* strains (Thomas *et al.*, 2004; Korea *et al.*, 2011) and are potentially useful additions to the exoelectrogenic *E. coli* strain because these appendages have naturally evolved to mediate attachment with low impact on other outer membrane functions. Here, we explore the possibility of obtaining an exoelectrogenic biofilm-forming *E. coli* variant by production of mannose specific Fim pili and report the effect of pili production on the cytochrome production levels, the exoelectrogenic performance and its adhesive properties with respect to Fim ligands and an electrode surface.

Results and discussion

Design of *E. coli* coproducing *CymAMtrCAB* and *FimAICDFGH* for the biochemical characterization of Fim pili and the METP

In order to test whether functional Fim pili and the METP comprising the *S. oneidensis* electron transfer proteins CymA and MtrCAB can be coproduced in *E. coli*, a set of four *E. coli* strains was constructed (Table 1). This included a reference strain, called *cymA-mtr-Sm^R*, which was prepared from the existing exoelectrogenic *E. coli* strain *cymA-mtr* (TerAvest *et al.*, 2014) by transformation with the insert-free expression vector pCDFDuet-1. In addition to pCDFDuet-1, this *E. coli* strain contained the vectors pEC86 and I5049, which are required for the efficient production of the *S. oneidensis* electron conduit in *E. coli*. The recombinantly expressed genes comprised the *E. coli* cytochrome *c* maturation genes *ccmA-H*, which were incorporated in the pEC86 construct under the control of the constitutive *tet* promoter. The *cymAmtrCAB* gene cluster was placed downstream of the IPTG-inducible T7/*lac* promoter in plasmid I5049. Three additional *E. coli* strains were prepared in order to investigate whether functional Fim pili can be produced in the studied *E. coli* system and distinguished from the non-piliated phenotype. These strains were designed to either coproduce Fim pili and CymAMtrCAB (strain *cymA-mtr-fim*), to exclusively produce Fim pili as heterologous membrane protein (strain *fim-Kan^R*) or not to produce any heterologous cell envelope proteins at all (strain *Kan^R-Sm^R*). All these strains carried three different plasmids of which the *ccmA-H* expression construct pEC86 was included in every strain. In addition, *Kan^R-Sm^R* control strains *Kan^R-Sm^R* and *fim-Kan^R* contained the empty pET30a+ derivative pSB1ET2 while the strains *cymA-mtr-Sm^R* and *cymA-mtr-fim* carried the pSB1ET2

derivative I5049 with added *cymAmtrCAB* gene insert under the control of the T7/*lac* promoter. Non-piliated control strains (*Sm^R*) harboured the insert-free expression construct pCDFDuet-1 and pilated *fim* strains contained the pCDFDuet-1 derivative pMil20. This plasmid included the Fim pili gene cluster *fimAICDFGH* inserted downstream of the IPTG-inducible T7/*lac* promoter.

Recombinant Fim pili production attenuates CymA concentration but imposes little stress on exoelectrogenic *E. coli*

The heterologous production of recombinant outer membrane proteins in the host *S. oneidensis* has been reported to adversely affect the production of the outer membrane protein complex MtrCAB (Kane *et al.*, 2013). To test whether this is also true in the case of added Fim pili in the exoelectrogenic *E. coli* strains, we cultivated the four *E. coli* strains *Kan^R-Sm^R*, *fim-Kan^R*, *cymA-mtr-Sm^R* and *cymA-mtr-fim* in BES's under anaerobic conditions overnight at a working electrode potential of +200 mV versus Ag/AgCl. Samples were taken from the BES and analysed with regard to the cell content of type I pili components using immunoblotting (FimCH) and electron transfer proteins using enhanced chemiluminescence (CymA, MtrA and MtrC). A comparison of the FimC and FimH production levels in the whole cell lysates of two *fim* strains revealed that intensity of both proteins was lower when the METP genes were coexpressed (Fig. 2A). Similarly, analysis of the *c*-type cytochromes revealed that CymA levels were clearly decreased while MtrC and MtrA levels were largely unchanged when compared to the strain lacking the *fim* gene cluster (Fig. 2B). We speculate that the decrease in relative expression levels is due to a limited overall production capacity for membrane proteins. The stress imposed on the exoelectrogenic *E. coli* cell by

Table 1. Bacterial strains produced in the present study. All strains are derivatives of the *E. coli* cell line C43(DE3).

<i>E. coli</i> strain	Plasmids ^a	VTT Culture collection ID
<i>Kan^R-Sm^R</i>	pEC86 (<i>ccmA-H</i>), pSB1ET2 (-), pCDFDuet-1 (-)	E-183553
<i>cymA-mtr-Sm^R</i>	pEC86 (<i>ccmA-H</i>), I5049 (<i>cymAmtrCAB</i>), pCDFDuet-1 (-)	E-183554
<i>fim-Kan^R</i>	pEC86 (<i>ccmA-H</i>), pSB1ET2 (-), pMil20 (<i>fimAICDFGH</i>)	E-183555
<i>cymA-mtr-fim</i>	pEC86 (<i>ccmA-H</i>), I5049 (<i>cymAmtrCAB</i>), pMil20 (<i>fimAICDFGH</i>)	E-183556

a. Inducible genes stated in brackets with '-' denoting an insert-free vector.

recombinantly produced pili and electron transfer proteins was monitored through the rate of growth at 37°C. These experiments showed that there was no measurable difference in growth rate between the control strain Kan^R-Sm^R and the Fim pili gene expressing strain *fim*-Kan^R (Appendix S1). In the presence of cytochrome genes, a 20% decreased growth rate was measured when compared to the *E. coli* strains lacking the METP genes. These data indicate that the production of the *S. oneidensis* electron transfer components is a larger energetic burden to the *E. coli* cell than the production of *E. coli* Fim pili.

Fim gene expression increases binding to mannose-coated surfaces

The mannose specific binding of the *E. coli* strains was studied as adsorption to mannose-functionalized agarose beads. Microscopy images reveal attached cells in the case of *fim* strains as apparent for strain *fim*-Kan^R (Fig. 3A and B). The variant *cymA-mtr-fim* formed slightly less dense cell layers, while almost no attachment of cells was observed in the case of the non-piliated control strains Kan^R-Sm^R and *cymA-mtr*-Sm^R (Fig. 3C). These experiments showed that mannose-binding Fim pili can be produced in the exoelectrogenic *E. coli* system and that the two *E. coli* *fim* strains form biofilms on mannose with no significant background binding.

The capacity of the METP to reduce soluble substrates is preserved during pili coproduction

The effect of pili coproduction on the Mtr electron transfer functionality was measured using a soluble Fe(III) reduction assay. This was done using cells of all four *E. coli* strains that were, prior to this reduction assay, incubated overnight in an anaerobic BES at a working electrode potential of +200 mV versus Ag/AgCl. The observed Fe(II) formation indicated that the two *cymA-mtr* strains were performing the Fe(III) reduction at identical rates that were significantly above the apparent background reduction activity as measured in M1 medium (Fig. 4). The Fe(III)-reductive activity of both Kan^R-control strains was identical to the background activity, which confirmed that this assay specifically measures the activity of the METP. Based on the differential CymA production (Fig. 2B), the unchanged ferric citrate reduction rate of *cymA-mtr-fim* when compared to the non-piliated strain *cymA-mtr*-Sm^R is an unexpected result. The apparent tolerance of the exoelectrogenic *E. coli* to decreased CymA levels may be due to the presence of the native inner membrane cytochrome NapC which has been proposed to fulfil the same EET function as CymA (Jensen *et al.*, 2016). These data suggest that Fim pili and the METP can be coproduced without affecting the capability of the cell to reduce soluble electron acceptors.

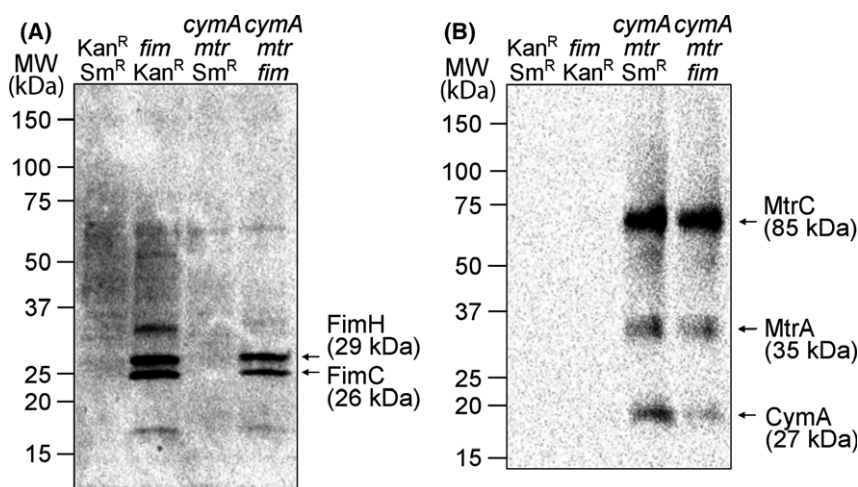


Fig. 2. Analysis of recombinant protein levels in *E. coli* strains using SDS-PAGE (4–20% polyacrylamide gradient) and Western blot analysis. The analysed cell lysates were prepared from strains that either did not contain *S. oneidensis* EET components or pili genes (Kan^R-Sm^R), the Fim pili gene cluster *fimAICDFGH* but no encoded *S. oneidensis* EET components (*fim*-Kan^R), no Fim pili genes but the *S. oneidensis* EET component gene cluster *cymAmtrCAB* (*cymA-mtr*-Sm^R) or both, pili and *S. oneidensis* EET component gene clusters (*cymA-mtr-fim*). The cells were collected following an overnight incubation in a BES at a E_{WE} of +200 mV versus Ag/AgCl. The separated cell lysates were labelled with rabbit antibodies specific for Fim pili components FimC and FimH (A). Bound antibodies were visualized by enhanced chemiluminescence following addition of horseradish peroxidase-conjugated secondary antibodies (A). In subfigure B, redox-active cytochromes CymA, MtrA and MtrC were detected directly by enhanced chemiluminescence. The positions of molecular weight standard proteins, the predicted positions of the antibody labelled proteins (A) and haem-containing proteins (B) along with their molecular weights are indicated.

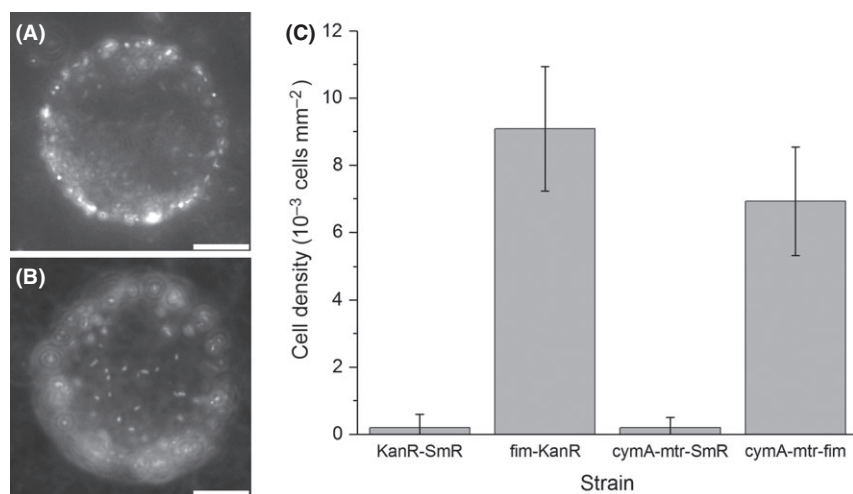


Fig. 3. Mannose-binding assay investigating binding of the *E. coli* strains $\text{Km}^{\text{R}}\text{-Sm}^{\text{R}}$, $\text{fim-Kan}^{\text{R}}$, $\text{cymA-mtr-Sm}^{\text{R}}$ and cymA-mtr-fim to mannose-coated agarose beads. A dense corona of propidium iodide-stained *E. coli* $\text{fim-Kan}^{\text{R}}$ cells is apparent at the bead centre focus and at the top pole focus (A and B, respectively; 20 μm scale bar). A comparison of cell binding as determined from top bead poles (C) reveals that both pili-producing strains $\text{fim-Kan}^{\text{R}}$ and cymA-mtr-fim bound to the mannose beads at high densities of $> 5 \times 10^3$ cells mm^{-2} while no significant attachment was measured with strains $\text{Km}^{\text{R}}\text{-Sm}^{\text{R}}$ and $\text{cymA-mtr-Sm}^{\text{R}}$. For each strain, the density of bound cells was determined from five beads with similar diameter of around 100 μm . The imaged spherical cap area was determined from the bead diameter and the assayed projected cap area.

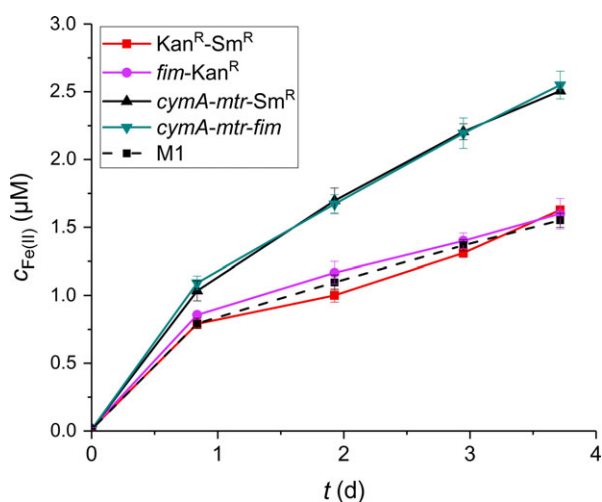


Fig. 4. Ferric iron reduction measured by the ferrozine method in M1 medium without cells (M1) and in the presence of cells of *E. coli* strains $\text{Kan}^{\text{R}}\text{-Sm}^{\text{R}}$, $\text{fim-Kan}^{\text{R}}$, $\text{cymA-mtr-Sm}^{\text{R}}$ and cymA-mtr-fim . The M1 medium was supplemented with 10 mM Fe(III) citrate and 40 mM lactate. During overnight incubation prior to supplement addition, the bacterial cells were exposed to an E_{WE} of +200 mV versus Ag/AgCl. Displayed are averages of triplicate measurements with the corresponding standard deviation as error bars.

E. coli producing type 1 pili and the METP produce current and show increased persistence in BESs

Lactate cannot be fermented by *E. coli* and was therefore chosen as a substrate to test the ability of the cell to transfer electrons released from substrate oxidation to an extracellular electrode. The current response was

monitored by chronoamperometry for at least 50 h following addition of lactate [40 mM]. The initial lactate concentration was chosen based on previous studies in which the exoelectrogenic *E. coli* system produced a clear electric signal under similar conditions (TerAvest *et al.*, 2014). The cytochrome-free strains $\text{fim-Kan}^{\text{R}}$ and $\text{Kan}^{\text{R}}\text{-Sm}^{\text{R}}$ produced constant currents throughout the measured interval with current densities of 0.70 ± 0.08 and 1.09 ± 0.07 $\mu\text{A cm}^{-2}$ respectively (Fig. 5). Those background currents may be related to hydroquinone derivatives that have previously been proposed to be produced by *E. coli* cells and which may act as mediators of extracellular electron transport (Qiao *et al.*, 2011). The highest electroactivity was measured with the cytochrome producing strain $\text{cymA-mtr-Sm}^{\text{R}}$ that started with a current density of 3.6 $\mu\text{A cm}^{-2}$ followed by a steady increase to a maximum current density of 4.5 $\mu\text{A cm}^{-2}$ over a 28 h period after which the current decreased to 4.0 $\mu\text{A cm}^{-2}$ by the end of the experiment. The current density produced by the strain which coproduced pili and cytochromes increased from 1.8 $\mu\text{A cm}^{-2}$ to a maximum of 1.9 $\mu\text{A cm}^{-2}$ during 20 h and decreased to a level of 1.7 $\mu\text{A cm}^{-2}$ at 55 h past lactate addition. Monitoring of the lactate concentration by HPLC analysis showed that all tested strains consumed only a small fraction of the added lactate substrate during the electrocultivation, which is consistent with predictions based on the observed electric currents and showed that the availability of this substrate was not limiting metabolic activity. The current produced by strain cymA-mtr-fim was significantly higher than the current of 1.07 $\mu\text{A cm}^{-2}$

that was measured with the most electroactive non-Mtr control strain Kan^R-Sm^R (Fig. 5, Appendix S2; $P = 0.018$; two-tailed Student's *t*-test).

Interestingly, the current produced by *E. coli cymA-mtr-fim* was 58% lower than the electric current measured with the non-piliated form (i.e. *cymA-mtr*-Sm^R: $4.0 \mu\text{A cm}^{-2}$). The ferric citrate reduction assay has shown that this current decrease is not due to a METP disruption. We speculate that this effect is due to steric restrictions of attractive electrode–cell interactions that are imposed by Fim pili and lead to a reduction in outer membrane cytochromes (such as MtrC) that are close enough to the electrode surface to participate in direct electron transfer. This hypothesis is supported by the observation that cell suspensions of both *fim* strains do not sediment upon static incubation at room temperature whereas both Sm^R strains settle out of the fluid under these conditions (data not shown). A similar phenomenon has been reported by Meuskens *et al.* (2017) who have observed increased flocculation of *E. coli* strains which lacked several outer membrane proteins. As an explanation, the authors proposed a shielding function of outer membrane proteins that controls aggregation by limiting electrostatic attraction between cells. Such charge shielding may also limit electron transfer to the carbon electrode in the exoelectrogenic *E. coli* system but does, as is apparent from the unchanged ferric iron reduction, not affect the electron transfer to soluble electron acceptors. The small size of the ferric iron anion may allow it to penetrate the pili layer and support EET in pili-producing cells at the same rate as in non-piliated cells. The shielding effects of pili may be mitigated by

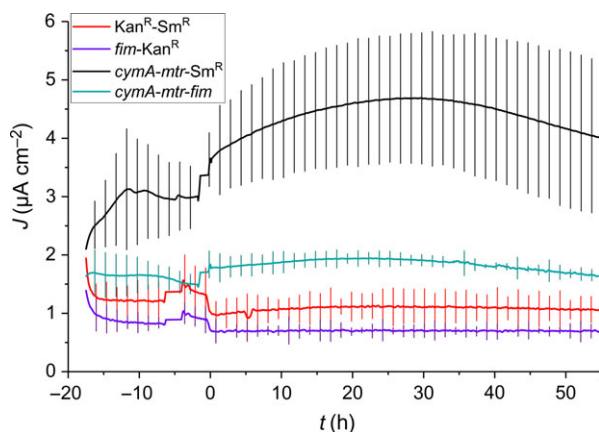


Fig. 5. Chronoamperometry analysis of *E. coli* strains Kan^R-Sm^R, *fim*-Kan^R, *cymA-mtr*-Sm^R and *cymA-mtr-fim* interacting with a carbon cloth working electrode poised at $E_{WE} = +200$ mV versus Ag/AgCl. Lactate was added at $t = 0$ h to a final concentration of 40 mM following an 18-h precultivation without carbon source. Error bars indicate standard error of triplicate measurements.

usage of a more tunable induction system for pili gene expression.

Exoelectrogenic *E. coli* cells spontaneously adsorb to carbon electrodes as thin layers and since type I pili promote the aggregation of *E. coli* cells (Ogden and Taylor, 1991), we hypothesized that the thickness of a spontaneously adsorbed exoelectrogenic biofilm could be increased by expression of *fim* genes. To test this, we measured the biomass present in solution and on the anode surface after 5 days in the BESs. Examination of anode-bound biomass and biomass in solution shows that, while there are no significant differences in the solution biomass among the different strains, there is a significant ~2.5-fold increase in anode-bound biomass in the *cymA-mtr-fim* strain relative to the strains Kan^R-Sm^R and *fim*-Kan^R (10.28 ± 1.66 mg versus 3.69 ± 0.50 mg and 3.31 ± 0.21 mg, $P = 0.003$ and 0.002 , respectively; two-tailed Student's *t*-test; comparison presented in Appendix S2). This observation indicates that, unlike adhesion to mannose-coated surfaces, *fim* expression alone was insufficient to significantly increase cell biomass on the anode. Rather, both Fim pili and the METP were required to enhance cell binding to the anode.

The exact mechanism through which the METP promotes cell adhesion is not evident from the presented data but may be linked to the cellular anodic respiration, which can only occur while the bacterial cell is in contact with the electrode. The Kan^R strains exhibited 40% background adsorption to carbon cloth, whereas no significant background adhesion was measured with the strains *cymA-mtr*-Sm^R and Kan^R-Sm^R on mannose. This indicates that utilization of Fim pili based carbohydrate binding for immobilization of exoelectrogenic cells is preferable over cytochrome mediated adsorption to carbon and a promising approach to achieve specific binding at solid surfaces. For this approach, the carbon electrode has to be modified with mannose groups which has been achieved previously by carbodiimide coupling of amino-functionalized mannose to a carboxylated carbon electrode substrate (Gu *et al.*, 2008; Ehlert *et al.*, 2011). Carbohydrates may also be immobilized on gold (He *et al.*, 2011), which, based on its low resistance and inertness, appears as an interesting alternative to carbon in biosensing applications. However, gold is prone to spontaneous protein adsorption (De Paoli Lacerda *et al.*, 2010), which may prevent specific cell adhesion and external electron transfer.

Coproduction of the METP and cell adhesion proteins in *E. coli* offers new opportunities for bioelectronic applications

The presented exoelectrogenic *E. coli* strain may be developed further for bioelectronic applications that

demand both, specific surface binding and higher EET rate by introduction of genetic modifications that result in a lower pili density and thereby improve the electron transfer through the extracellular space. Furthermore, the EET efficiency of this strain could be improved by utilization of the currently known conductive pili (Holmes *et al.*, 2016) by, for instance, coproduction of conductive and adhesive pili in the same cell or by replacing the Fim pili with novel rationally designed hybrid pili that consist of a long conductive fibre and a terminal carbohydrate-binding adhesin. Alternatively, the EET of *E. coli cymA-mtr-fim* could be promoted through penetration of the pili layer with electrode-tethered conductive polymers such as linear naphthoquinone-modified polyethylenimine hydrogels through which electrons can be transferred by shuttling between the covalently bound redox centres (Milton *et al.*, 2015).

Among the selective cell adhesion systems found in nature, the adhesin/lectin–carbohydrate system is most common and includes a wide range of ligand–receptor pairs. In addition to this approach, other strategies have been employed, like, for example, biofilm patterning with a genetically engineered *E. coli* strain that adsorbed to various substrates with Ag43 adhesin upon illumination (Jin and Riedel-Kruse, 2018). The Ag43 adhesin system is, however, considered disadvantageous for the proposed signal multiplexing because it is non-specific and therefore incompatible with selective binding of different types of cells from a mixture. Other cell adhesion systems with technical relevance include, the cell binding by cell-surface bound antibody targets (Suo *et al.*, 2008) and recombination of protein dimer components exposed at the outer cell membrane and the adhesion substrate (Chen and Wegner, 2017).

Existing electroactive biosensing applications, relevant for the exoelectrogenic *E. coli* system, include predominantly multispecies systems that were designed for monitoring of process parameters such as the oxygen demand, the production of volatile fatty acids and presence of toxins (Modin and Aulenta, 2007). In addition, several single-species sensing systems have been developed for, for example, monitoring of acetate by *G. sulfurreducens* (Tront *et al.*, 2008; Nevin *et al.*, 2011), sensing of lactate, fumarate and arabinose by *S. oneidensis* (Kouzuma *et al.*, 2012; Golitsch *et al.*, 2013; Si *et al.*, 2015) and the detection of arsenic by *Enterobacter cloacae* and *S. oneidensis* (Webster *et al.*, 2014; Rasmussen and Minter, 2015). More advanced applications include the cell-internal processing of quorum sensing signals which has been achieved by the creation of AND logic gates in *S. oneidensis* and *P. aeruginosa* (Li *et al.*, 2011; Hu *et al.*, 2015). The performance of biosensors will benefit from miniaturization, for example, sensing in microfluidic systems. The coproduction of

METP and adhesive pili is a novel strategy with which electroactive cells can be targeted to inorganic surfaces and is therefore a promising approach for the realization of such patterned bioelectronics.

Experimental procedures

Strains and plasmids

Information on the plasmids, bacterial strains and primers used in this study is given in Table 1 and Appendix S3–S5. The plasmid pMil020 for recombinant Fim pili production was constructed by subcloning the *fim* operon as two PCR fragments from pSH2 (courtesy of Prof. Paul Orndorff) (Orndorff and Falkow, 1984). The *fimAICD* gene fragment was amplified and extended with a 5'-terminal restriction site using the PCR primers *NdeI_fim_fw1* and *SH2_27_rv*. The *fimDFGH* gene fragment was amplified with a 3'-terminal *AvrII* restriction site using the primers *SH2_24_fw* and *AvrII_fimH_rv1*. Both fragments were cloned into pCR2.1-TOPO vectors (*fimAICD*: pCR2.1-TOPO+PCR4-c6; *fimDFGH*: pCR2.1-TOPO+PCR5-c6) using the TOPO TA cloning kit (Thermo Fisher Scientific, Waltham, MA, USA) and confirmed by sequencing. The vectors pCR2.1-TOPO+PCR4-c6 and pCR2.1-TOPO+PCR5-c6 were subjected to *NdeI*–*BamHI* and *BamHI*–*AvrII* digest to yield *fimAICD* and *fimDFGH* fragments respectively. The vector pCDFDuet-1 was double-digested using restriction enzymes *NdeI* and *AvrII*, and the resulting large vector fragment was ligated with the purified *fimAICD*- and *fimDFGH* fragments yielding the expression construct pMil020 (Appendix S3 and S4). The correct assembly was confirmed by sequencing. An *E. coli* XL-1 Blue strain harbouring the plasmid pMil20 was deposited with the VTT Culture Collection (strain ID E-183557) as well as the presented *E. coli* C43(DE3) strain variants Kan^R-Sm^R (strain ID E-183553), *fim*-Kan^R (strain ID E-183555), *cymA-mtr*-Sm^R (strain ID E-183554) and *cymA-mtr-fim* (strain ID E-183556) (see Table 1).

Culture conditions

Prior to BES cultivation, bacterial cells were grown overnight at 37°C and 220 rpm in 5 mL 2×YT broth (16 g l⁻¹ tryptone, 10 g l⁻¹ yeast extract, 5 g l⁻¹ NaCl, pH 7.0, supplemented with 50 µg ml⁻¹ kanamycin, 100 µg ml⁻¹ chloramphenicol and 50 µg ml⁻¹ streptomycin). Then, 500 µl preculture was added to 50 ml 2×YT broth and incubated at 30°C and 220 rpm until an OD_{595 nm} of 0.5–0.9 was reached. The inducer isopropyl β-D-1-thiogalactopyranoside (IPTG) was then added to a final concentration of 50 µM. The production of recombinant proteins was allowed for about 20 h at a reduced agitation of 200 rpm. Cell cultures harbouring the I5049

vector were supplemented with the haem precursor δ -aminolevulinic acid at a final concentration of 1 mM in order to enhance haem biosynthesis and optimal cytochrome production (Fernandes *et al.*, 2008).

Detection of Fim pili component and cytochrome production by Western blot analysis

Frozen *E. coli* cell samples were thawed and resuspended in B-PER bacterial protein extraction reagent (Thermo Fisher Scientific) at an OD_{595 nm} of 3.5. The following components were added at the given final concentrations: 1.0 mM EDTA, 4.2 mM MgCl₂, 12 $\mu\text{g ml}^{-1}$ chicken egg lysozyme, 10 $\mu\text{g ml}^{-1}$ DNase I and 1.0 mM PMSF. The lysis reaction was performed at room temperature for 1 h followed by separation of the protein components in the lysed sample by reducing (analysis of Fim pili components) or non-reducing (analysis of cytochromes) SDS-PAGE (4–20% polyacrylamide gradient). The separated proteins were blotted onto nitrocellulose. Pili components FimC and FimH were labelled with a FimCH specific rabbit primary antibody (courtesy of David G. Thanassi) at a working dilution of 1:50 000. Primary antibody binding was detected by enhanced chemiluminescence using a rabbit-IgG-(H+L) specific antibody that was conjugated to horseradish peroxidase (Rockland Immunochemicals, Limerick, PA, USA) and reacted with SuperSignal West Pico chemiluminescent substrate (Thermo Fisher Scientific). The cytochrome detection was carried out by exposing the nitrocellulose membrane directly to the chemiluminescent substrate as previously described by Vargas *et al.* (1993).

Mannose-binding assay

Functional Fim pili production was monitored using a mannose-binding assay. *E. coli* cultures in which recombinant gene transcription was induced with IPTG (see above) were collected by centrifugation (15 min at 4°C and 3200 *g*) and resuspended in M1 medium (see Appendix S6). D-mannose-coated agarose beads ($\text{\O} = 52\text{--}165 \mu\text{m}$; bioWORLD, Dublin, OH, USA) were washed twice with ddH₂O and thrice with M1 medium (seven bead volumes, each). Washed beads ($V = 5.5 \mu\text{l}$) were combined with the cell suspension in microtitre plate wells and diluted with M1 medium to OD_{595 nm} = 0.2 ($V_{\text{Total}} = 200 \mu\text{l}$ per well). The plate was sealed and incubated for 1 h at 37°C followed by sedimentation of the beads for 5 min at 22°C and 400 *g*. The supernatant was replaced with sterile M1 medium and the plate was incubated overnight at 22°C. Bacterial cells were fluorescently stained by addition of 0.3 μl propidium iodide solution (20 mM in DMSO) to each microtitre plate well and a 15-min incubation at 22°C in the

dark. The reaction liquid was replaced with M1 medium and cell binding examined at $\lambda_{\text{Ex}} = 520\text{--}550 \text{ nm}$ using an IX81 inverted microscope (Olympus, Tokyo, Japan).

Soluble Fe(III) reduction assay

All preparative steps of this method were performed in an anaerobic cabinet (80% N₂, 10% CO₂, 10% H₂). Cells suspended in M1 medium containing lactate [40 mM] were diluted to OD_{595 nm} = 0.5 using the same medium. Fe(III) citrate was added to the cells at a final concentration of 10 mM and the Fe(II) concentration was monitored by daily sampling. Fe(II) in 50 μl aliquots was acid extracted for 1 h in 0.5 mL 0.5 M HCl. The Fe(II) concentration was determined using a modified method from L. Stookey (Stookey, 1970) according to which 50 μl of the acid extract was added to 1.0 mL ferrozine solution ($c = 1.0 \text{ M}$; dissolved in 0.1 M HEPES, pH 8.0) and left to react for 10 min. The concentration of the Fe(II)-(ferrozine)₃⁴⁻ complex was determined from A_{563 nm} ($\epsilon_{563 \text{ nm}} = 27.9 \text{ mM}^{-1} \text{ cm}^{-1}$) of 200- μl reaction volumes using a Varioskan microtitre plate reader (Thermo Fisher Scientific).

BES setup

The voltammetry cells were assembled according to the setup described earlier by Marsili *et al.* (2008b) with slight modifications. In detail, the setup comprised a 6.4-cm²-sized rectangular carbon cloth working electrode (Panex 30-SW08; Zoltek, Nyergesújfalú, Hungary) which was cleaned by incubation in 1 M NaOH, 1 M HCl, acetone (2 \times) and ddH₂O (2 \times) and attached to a custom-made polyether ether ketone barrel ($\text{\O} = 9 \text{ mm}$) using Pt wire ($\text{\O} = 0.05 \text{ mm}$). The cell lid was manufactured in-house from Teflon, and the remaining components were purchased from Bioanalytical systems (West Lafayette, IN, USA) including a MR-1194 voltammetry cell, a MW-4130 Pt wire counter electrode ($\text{\O} = 0.05 \text{ mm}$) and an MF-2079 Ag/AgCl reference electrode that was contained in a MF-2031 glass chamber, capped with a MF-2064 Vycor frit and filled with 0.1 M NaCl. The assembled BES was sterilized by autoclaving without the Ag/AgCl reference electrode. After growth, the IPTG-induced cells were collected by centrifugation (2450 *g*, 15 min, 4°C) and washed three times in 20 mL ice-cold M1 medium. The cells were resuspended in 10 mL and diluted to OD_{595 nm} = 1.0 in a final volume of 60 mL using M1 medium as diluent. The remaining cells were collected by centrifugation (2450 *g*, 15 min, 4°C) and stored as a frozen pellet for Western blot analysis. For electrochemical measurements, 60 mL cell suspension was transferred into each BES, stirred at 200 rpm, maintained at 30°C and sparged with a humidified anoxic

atmosphere (80% N₂, 20% CO₂) at a flow rate of 5 ml min⁻¹.

Electrochemical measurements

Chronoamperometry experiments were executed using a WaveNow potentiostat (Pine Research Instrumentation, Durham, NC, USA).

Acknowledgements

This research has been financially supported through the VTT Frontier Programme, the Biosolar programme granted by Tekes – the Finnish Funding Agency for Innovation (Diary No. 2299/31/2012; Decision No. 40044/13) and the Academy of Finland through a post-doctoral research grant (Decision No. 277121 to ML) and research grants SYNECO2 (Decision No. 272569 to JJ) and OPTOBIO (Decision No. 287011 to MP). Work at the Molecular Foundry was supported by the Office of Science, Basic Energy Sciences programme of the U.S. Department of Energy (Contract No. DE-AC02-05CH11231). CMAF and MAT acknowledge support from Office of Naval Research (Award number N000141310551). Dr. Heather M. Jensen, Matt Hepler, Cheryl P. Goldbeck and Dr. Behzad Rad are thanked for supporting this research at the LBNL through advice and practical help. The authors would like to thank Prof. Paul Orndorff at North Carolina State University for generously providing the pSH2 plasmid, and Prof. David Thanassi as well as Nadine Henderson at Stony Brook University for their generous gift of Fim pili specific antibodies. We are grateful to Dr. Jörg Deutzmann for a critical review of the manuscript.

Conflicts of interests

We declare that there are no conflicts of interests regarding the publication of this manuscript.

References

Breuer, M., Rosso, K.M., Blumberger, J., and Butt, J.N. (2015) Multi-haem cytochromes in *Shewanella oneidensis* MR-1: structures, functions and opportunities. *J Royal Soc Interface* **12**: 20141117.

Brutinel, E.D., and Gralnick, J.A. (2012a) Preferential utilization of D-Lactate by *Shewanella oneidensis*. *Appl Environ Microbiol* **78**: 8474–8476.

Brutinel, E.D., and Gralnick, J.A. (2012b) Shuttling happens: soluble flavin mediators of extracellular electron transfer in *Shewanella*. *Appl Microbiol Biotechnol* **93**: 41–48.

Chen, F., and Wegner, S.V. (2017) Blue light switchable bacterial adhesion as a key step toward the design of biofilms. *ACS Synth Biol* **6**: 2170–2174.

Cordova, C.D., Schicklberger, M.F.R., Yu, Y., and Spormann, A.M. (2011) Partial functional replacement of CymA by SirCD in *Shewanella oneidensis* MR-1. *J Bacteriol* **193**: 2312–2321.

Coursolle, D., and Gralnick, J.A. (2010) Modularity of the Mtr respiratory pathway of *Shewanella oneidensis* strain MR-1. *Mol Microbiol* **77**: 995–1008.

De Paoli Lacerda, S.H., Park, J.J., Meuse, C., Pristinski, D., Becker, M.L., Karim, A., and Douglas, J.F. (2010) Interaction of gold nanoparticles with common human blood proteins. *ACS Nano* **4**: 365–379.

Ehlert, G.J., Lin, Y., and Sodano, H.A. (2011) Carboxyl functionalization of carbon fibers through a grafting reaction that preserves fiber tensile strength. *Carbon* **49**: 4246–4255.

Fernandes, A.P., Couto, I., Morgado, L., Londer, Y.Y., and Salgueiro, C.A. (2008) Isotopic labeling of c-type multi-heme cytochromes overexpressed in *E. coli*. *Protein Expr Purif* **59**: 182–188.

Firer-Sherwood, M.A., Bewley, K.D., Mock, J.-Y., and Elliott, S.J. (2011) Tools for resolving complexity in the electron transfer networks of multiheme cytochromes c. *Metalomics* **3**: 344–348.

Fonseca, B.M., Paquete, C.M., Neto, S.E., Pacheco, I., Soares, C.M., and Louro, R.O. (2013) Mind the gap: cytochrome interactions reveal electron pathways across the periplasm of *Shewanella oneidensis* MR-1. *Biochem J* **449**: 101–108.

Förster, A.H., Beblawy, S., Golitsch, F., and Gescher, J. (2017) Electrode-assisted acetoin production in a metabolically engineered *Escherichia coli* strain. *Biotechnol Biofuels* **10**: 65.

Gescher, J., Cordova, C.D., and Spormann, A.M. (2008) Dissimilatory iron reduction in *Escherichia coli*: identification of CymA of *Shewanella oneidensis* and NapC of *E. coli* as ferric reductases. *Mol Microbiol* **68**: 706–719.

Goldbeck, C.P., Jensen, H.M., TerAvest, M.A., Beedle, N., Appling, Y., Hepler, M., Cambay, G., Mutalik, V., Angenent, L.T. and Ajo-Franklin, C.M. (2013) Tuning promoter strengths for improved synthesis and function of electron conduits in *Escherichia coli*. *ACS Synth Biol* **2**: 150–159.

Golitsch, F., Bücking, C., and Gescher, J. (2013) Proof of principle for an engineered microbial biosensor based on *Shewanella oneidensis* outer membrane protein complexes. *Biosens Bioelectron* **47**: 285–291.

Gu, L., Luo, P.G., Wang, H., Meziani, M.J., Lin, Y., Veca, L.M., Cao, L., Lu, F., Wang, X., Quinn, R.A., Wang, W., Zhang, P., Lacher, S. and Sun, Y.-P. (2008) Single-walled carbon nanotube as a unique scaffold for the multivalent display of sugars. *Biomacromol* **9**: 2408–2418.

He, X.-P., Wang, X.-W., Jin, X.-P., Zhou, H., Shi, X.-X., Chen, G.-R., and Long, Y.-T. (2011) Epimeric monosaccharide-quinone hybrids on gold electrodes toward the electrochemical probing of specific carbohydrate–protein recognitions. *Proc Natl Acad Sci USA* **133**: 3649–3657.

Holmes, D.E., Dang, Y., Walker, D.J.F. and Lovley, D.R. (2016) The electrically conductive pili of *Geobacter* species are a recently evolved feature for extracellular electron transfer. *Microb Genom* **2**, e000072.

Hu, Y., Yang, Y., Katz, E., and Song, H. (2015) Programming the quorum sensing-based AND gate in *Shewanella*

- oneidensis* for logic gated-microbial fuel cells. *Chem Commun* **51**: 4184–4187.
- Jensen, H.M., Albers, A.E., Malley, K.R., Londer, Y.Y., Cohen, B.E., Helms, B.A., Weigele, P., Groves, J.T. and Ajo-Franklin, C.M. (2010) Engineering of a synthetic electron conduit in living cells. *Proc Natl Acad Sci USA* **107**: 19213–19218.
- Jensen, H.M., TerAvest, M.A., Kokish, M.G., and Ajo-Franklin, C.M. (2016) CymA and exogenous flavins improve extracellular electron transfer and couple it to cell growth in Mtr-expressing *Escherichia coli*. *ACS Synth Biol* **5**: 679–688.
- Jin, X., and Riedel-Kruse, I.H. (2018) Biofilm Lithography enables high-resolution cell patterning via optogenetic adhesin expression. *Proc Natl Acad Sci USA* **115**: 3698–3703.
- Kane, A.L., Bond, D.R., and Gralnick, J.A. (2013) Electrochemical analysis of *Shewanella oneidensis* engineered to bind gold electrodes. *ACS Synth Biol* **2**: 93–101.
- Kane, A.L., Brutinel, E.D., Joo, H., Maysonet, R., VanDrusse, C.M., Kotloski, N.J., and Gralnick, J.A. (2016) Formate metabolism in *Shewanella oneidensis* generates proton motive force and prevents growth without an electron acceptor. *J Bacteriol* **198**: 1337–1346.
- Koch, C., and Harnisch, F. (2017) Is there a specific ecological niche for electroactive microorganisms? *ChemElectroChem* **3**: 1282–1295.
- Korea, C.G., Ghigo, J.M., and Beloin, C. (2011) The sweet connection: solving the riddle of multiple sugar-binding fimbrial adhesins in *Escherichia coli*. *BioEssays* **33**: 300–311.
- Kouzuma, A., Hashimoto, K., and Watanabe, K. (2012) Influences of aerobic respiration on current generation by *Shewanella oneidensis* MR-1 in single-chamber microbial fuel cells. *Biosci Biotechnol Biochem* **76**: 270–275.
- Kracke, F., Vassilev, I., and Krömer, J.O. (2015) Microbial electron transport and energy conservation – the foundation for optimizing bioelectrochemical systems. *Front Microbiol* **6**: 575.
- Li, Z., Rosenbaum, M.A., Venkataraman, A., Tam, T.K., Katz, E., and Angenent, L.T. (2011) Bacteria-based AND logic gate: a decision-making and self-powered biosensor. *Chem Commun* **47**: 3060–3062.
- Lovley, D.R. (1991) Dissimilatory Fe(III) and Mn(IV) reduction. *Microbiol Rev* **55**: 259–287.
- Lovley, D.R., and Phillips, E.J. (1988) Novel mode of microbial energy metabolism: organic carbon oxidation coupled to dissimilatory reduction of iron or manganese. *Appl Environ Microbiol* **54**: 1472–1480.
- Marritt, S.J., Lowe, T.G., Bye, J., McMillan, D.G., Shi, L., Fredrickson, J., Zachara, J., Richardson, D.J., Cheesman, M.R., Jeuken, L.J. and Butt, J.N. (2012) A functional description of CymA, an electron-transfer hub supporting anaerobic respiratory flexibility in *Shewanella*. *Biochem J* **444**: 465–474.
- Marsili, E., Baron, D.B., Shikhare, I.D., Coursolle, D., Gralnick, J.A., and Bond, D.R. (2008a) *Shewanella* secretes flavins that mediate extracellular electron transfer. *Proc Natl Acad Sci USA* **105**: 3968–3973.
- Marsili, E., Rollefson, J.B., Baron, D.B., Hozalski, R.M., and Bond, D.R. (2008b) Microbial biofilm voltammetry: direct electrochemical characterization of catalytic electrode-attached biofilms. *Appl Environ Microbiol* **74**: 7329–7337.
- Matias, V.R.F., Al-Amoudi, A., Dubochet, J., and Beveridge, T.J. (2003) Cryo-transmission electron microscopy of frozen-hydrated sections of *Escherichia coli* and *Pseudomonas aeruginosa*. *J Bacteriol* **185**: 6112–6118.
- Meshulam-Simon, G., Behrens, S., Choo, A.D., and Spormann, A.M. (2007) Hydrogen metabolism in *Shewanella oneidensis* MR-1. *Appl Environ Microbiol* **73**: 1153–1165.
- Meuskens, I., Michalik, M., Chauhan, N., Linke, D., and Leo, J. (2017) A new strain collection for improved expression of outer membrane proteins. *Front Cell Infect Microbiol* **7**: 464.
- Milton, R.D., Hickey, D.P., Abdellaoui, S., Lim, K., Wu, F., Tan, B., and Minteer, S.D. (2015) Rational design of quinones for high power density biofuel cells. *Chem Sci* **6**: 4867–4875.
- Modin, O., and Aulenta, F. (2007) Three promising applications of microbial electrochemistry for the water sector. *Environ Sci: Water Res Technol* **3**: 391–402.
- Nevin, K.P., Zhang, P., Franks, A.E., Woodard, T.L., and Lovley, D.R. (2011) Anaerobes unleashed: aerobic fuel cells of *Geobacter sulfurreducens*. *J Power Sources* **196**: 7514–7518.
- Ogden, K.L., and Taylor, A.L. (1991) Genetic control of flocculation in *Escherichia coli*. *J Ind Microbiol Biotechnol* **7**: 279–286.
- Orndorff, P.E., and Falkow, S. (1984) Organization and expression of genes responsible for type 1 piliation in *Escherichia coli*. *J Bacteriol* **159**: 736–744.
- Pinchuk, G.E., Rodionov, D.A., Yang, C., Li, X., Osterman, A.L., Dervyn, E., Geydebekht, O.V., Reed, S.B., Romine, M.F., Collart, F.R., Scott, J.H., Fredrickson, J.H. and Beliaev, A.S. (2009) Genomic reconstruction of *Shewanella oneidensis* MR-1 metabolism reveals a previously uncharacterized machinery for lactate utilization. *Proc Natl Acad Sci USA* **106**: 2874–2879.
- Pitts, K.E., Dobbin, P.S., Reyes-Ramirez, F., Thomson, A.J., Richardson, D.J., and Seward, H.E. (2003) Characterization of the *Shewanella oneidensis* MR-1 decaheme cytochrome MtrA: expression in *Escherichia coli* confers the ability to reduce soluble Fe(III) chelates. *J Biol Chem* **278**: 27758–27765.
- PrévotEAU, A., and Rabaey, K. (2017) Electroactive biofilms for sensing: reflections and perspectives. *ACS Sens* **2**: 1072–1085.
- Qiao, Y., Li, C.M., Bao, S.J., Lu, Z., and Hong, Y. (2011) Direct electrochemistry and electrocatalytic mechanism of evolved *Escherichia coli* cells in microbial fuel cells. *Chem Commun* **11**: 1290–1292.
- Rasmussen, M., and Minteer, S.D. (2015) Long-term arsenic monitoring with an *Enterobacter cloacae* microbial fuel cell. *Bioelectrochemistry* **106**: 207–212.
- Richter, K., Schicklberger, M., and Gescher, J. (2012) Dissimilatory reduction of extracellular electron acceptors in anaerobic respiration. *Appl Environ Microbiol* **78**: 913–921.
- Schuetz, B., Schicklberger, M., Kuermann, J., Spormann, A.M., and Gescher, J. (2009) Periplasmic electron transfer via the *c*-type cytochromes MtrA and FccA of *Shewanella oneidensis* MR-1. *Appl Environ Microbiol* **75**: 7789–7796.

- Si, R.-W., Zhai, D.-D., Liao, Z.-H., Gao, L., and Yong, Y.-C. (2015) A whole-cell electrochemical biosensing system based on bacterial inward electron flow for fumarate quantification. *Biosens Bioelectron* **68**: 34–40.
- Stookey, L.L. (1970) Ferrozine—a new spectrophotometric agent for iron. *Anal Chem* **42**: 779–781.
- Sturm-Richter, K., Golitsch, F., Sturm, G., Kipf, E., Dittrich, A., Beblawy, S., Kerzenmacher, S. and Gescher, J. (2015) Unbalanced fermentation of glycerol in *Escherichia coli* via heterologous production of an electron transport chain and electrode interaction in microbial electrochemical cells. *Bioresour Technol* **186**: 89–96.
- Suo, Z., Avci, R., Yang, X., and Pascual, D.W. (2008) Efficient immobilization and patterning of live bacterial cells. *Langmuir* **24**: 4161–4167.
- TerAvest, M.A., and Ajo-Franklin, C.M. (2016) Transforming exoelectrogens for biotechnology using synthetic biology. *Biotechnol Bioeng* **113**: 687–697.
- TerAvest, M.A., Zajdel, T.J., and Ajo-Franklin, C.M. (2014) The Mtr pathway of *Shewanella oneidensis* MR-1 couples substrate utilization to current production in *Escherichia coli*. *ChemElectroChem* **1**: 1874–1879.
- Thomas, W.E., Nilsson, L.M., Forero, M., Sokurenko, E.V., and Vogel, V. (2004) Shear-dependent 'stick-and-roll' adhesion of type 1 fimbriated *Escherichia coli*. *Mol Microbiol* **53**: 1545–1557.
- Tront, J.M., Fortner, J.D., Plötze, M., Hughes, J.B., and Puzrin, A.M. (2008) Microbial fuel cell biosensor for *in situ* assessment of microbial activity. *Biosens Bioelectron* **24**: 586–590.
- Vargas, C., McEwan, A.G., and Downie, J.A. (1993) Detection of c-type cytochromes using enhanced chemiluminescence. *Anal Chem* **209**: 323–326.
- Webster, D.P., TerAvest, M.A., Doud, D.F., Chakravorty, A., Holmes, E.C., Radens, C.M., Sureka, S., Gralnick, J.A. and Angenent, L.T. (2014) An arsenic-specific biosensor with genetically engineered *Shewanella oneidensis* in bio-electrochemical systems. *Biosens Bioelectron* **62**: 320–324.
- White, G.F., Edwards, M.J., Gomez-Perez, L., Richardson, D.J., Butt, J.N., and Clarke, T.A. (2016) Mechanisms of bacterial extracellular electron exchange. In *Advances in Bacterial Electron Transport Systems and Their Regulation*. Poole, R.K. (ed). Amsterdam: Elsevier Ltd., pp. 87–138.
- Xu, S., Jangir, Y., and El-Naggar, M.Y. (2016) Disentangling the roles of free and cytochrome-bound flavins in extracellular electron transport from *Shewanella oneidensis* MR-1. *Electrochim Acta* **198**: 49–55.

Supporting information

Additional supporting information may be found online in the Supporting Information section at the end of the article.

Appendix S1. Effect of the introduced recombinant genes on the growth of the tested *E. coli* strains.

Appendix S2. Biomass distribution and current density determined from BES cultivations of *E. coli* strain set.

Appendix S3. Plasmids used in this study.

Appendix S4. Map of vector pMil020.

Appendix S5. Primers used in this study.

Appendix S6. Composition of M1 medium.